

Features of the energy gap above T_c in $\text{Bi}_2\text{Sr}_2\text{CaCu}_2\text{O}_{8+\delta}$ as seen by break-junction tunneling

Toshikazu Ekino,* Yoshie Sezaki,[†] and Hironobu Fujii

Faculty of Integrated Arts and Sciences, Hiroshima University, Higashi-Hiroshima 739-8521, Japan

(Received 22 October 1998)

We report tunneling measurements of the energy gap above T_c using as-grown $\text{Bi}_2\text{Sr}_2\text{CaCu}_2\text{O}_{8+\delta}$ single crystals with $T_c = 86\text{--}89$ K, which are in slightly overdoped regions. The measurements were done with break junction for the temperatures mainly above 77 K at which the gap magnitudes of $4\Delta \approx 100$ meV are obtained. We find clear evidence for the gap above T_c . For the most significant data, the gap magnitude decreases with increasing the temperature up to T_c , but it turns to increase to reach ≈ 130 meV at $\approx 120\text{--}130$ K. The gap feature begins to reduce above this temperature and eventually disappears at the well-defined temperature of $T^* \approx 170\text{--}190$ K. The observation of the above characteristics is believed to be a consequence of the clean interface of the break junction, which enables us to probe delicate electronic structures in bulk $\text{Bi}_2\text{Sr}_2\text{CaCu}_2\text{O}_{8+\delta}$. [S0163-1829(99)02230-4]

Elucidation of the mechanism of high- T_c superconductivity should reveal an essential physics of the strongly-correlated conducting materials. Especially, the indication of the energy gap above the bulk superconducting critical temperature T_c has become one of the central interests for its unusual precursor effect.^{1,2,3} A remarkable progress has been made recently, namely, the gaplike feature above T_c was directly detected in $\text{Bi}_2\text{Sr}_2\text{CaCu}_2\text{O}_{8+\delta}$ (Bi-2212) by both photoemission and tunneling spectroscopies.^{4,5} This has been attributed to either the spin-singlet formation or the phase fluctuations of the pairing condensate.^{6,7} However, ambiguities still remain in determining the energy scales of the gap and its closing temperature among the different experiments.^{4,5} In this work we have done tunneling measurements of as grown Bi-2212 single crystals to address this issue. The electron tunneling technique provides a direct measurement of the quasiparticle density of states of a superconductor.⁸ Using this technique we find direct evidence for the gap creation at ≈ 190 K with the detailed temperature dependence of the gap. This feature would restrict the possible origins of the gap creation above T_c found in this compound.

Two kinds of the samples (no. 1 and no. 2) were grown by a standard flux method in 1 atm. air.⁹ The T_c 's were determined to be ≈ 86 K (no. 1)– 89 K (no. 2) as the zero-resistance temperature, which slightly depend on the crystal growth conditions. Judging from the ambient pressure during the crystal growth procedure and the measured T_c values, the samples are identified to be in the slightly overdoped regions.¹⁰ We used the break junction technique, in which very thin single crystal mounted on the glass-fiber substrate was cracked to form a junction at the low temperature by applying bending force perpendicular to the CuO_2 plane. This technique, giving *in situ* superconductor-insulator-superconductor (SIS) junction, has been quite effective to obtain clean and fresh interface. Usually the SIS junction is very sensitive to probe the gap-edge structure because of piling up of the densities of states of both sides of the junction barrier. Tunneling conductance, dI/dV , was measured using an ac modulation technique with four-probe method, where I and V are the current and the bias voltage across the junction, respectively.

Figure 1 shows the tunneling conductance dI/dV measured at 77.3 K from several different junctions made of two different crystal batches no. 1 (A, B, and D) and no. 2 (C). The high-bias junction resistances are in the range of $R_J \approx 10\ \Omega\text{--}3\ \text{k}\Omega$. A Josephson supercurrent is still visible at this temperature because of the SIS junction setup. The leakage conductance which is $\approx 60\text{--}70\%$ to the normal-state conductance except for D is fairly reproducible among the junctions. Judging from the intensive gap-edge peaks for this temperature, the leakage conductance arises not only from the density-of-states broadening but also from the nontunneling effect or the non-intrinsic tunneling from the possible off-stoichiometric region in the crystal. For the SIS junction

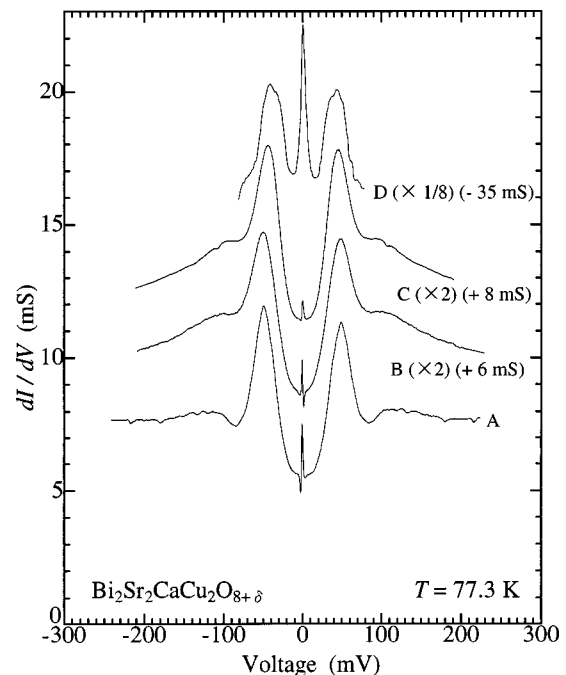


FIG. 1. Tunneling conductance from as-grown $\text{Bi}_2\text{Sr}_2\text{CaCu}_2\text{O}_{8+\delta}$ break junctions at 77.3 K. The sample batch is the same (no. 1) except for C (no. 2). The conductances are multiplied by the factors shown in the figure.

of a conventional superconductor, the *peak-to-peak* separation of dI/dV corresponds to $4\Delta(T)$,⁸ where $\Delta(T)$ is the gap parameter measured from the Fermi energy at a given temperature T . We adopt this definition here because no practical theory exists to determine the gap magnitude of the copper-oxide superconductors. The 4Δ (77.3 K) in this figure are 85–100 meV, but we have also observed much larger value of ≈ 130 meV using the samples from the same growth with the similar bulk T_c .¹¹ Since the distribution range is consistent with that of the other reports,^{12,13,14} it probably arises from uncontrollable local inhomogeneity in the sample. The valleys and subsequent broadened secondary peaks are seen just outside of the superconducting-gap peaks except for D . These features have been discussed in terms of the strong-coupling effect of the superconductivity,¹² while they are not observed in the other cuprates. It should be noted that the p - p energy separation ≈ 200 –250 meV of the above secondary peaks has been observed as a single gap by the break junction.¹¹ Therefore the secondary peaks in Fig. 1 can be attributed to the gap structure itself. In our preliminary measurements, the single gap having the above magnitude which corresponds to the secondary gap persists up to room temperature.¹¹ The energy scale of this secondary gap is close to the semiconducting gap associated with Bi_2O_2 layers.¹⁵ The details of this room-temperature gap are reported separately¹¹ because this issue is beyond the scope of this paper.

Figures 2 and 3 show the temperature variations of the tunneling conductance of Fig. 1 (A) and (C), respectively. It is obvious that the gap structure persists beyond $T_c \approx 86$ –89 K. These features give the main results of the paper, and the overall temperature behavior is reproduced in numbers of junctions.¹¹ The values of $R_J(200 \text{ mV}) \approx 130 \Omega$ and 420Ω at 77.3 K for Figs. 2 and 3, respectively, are much lower ($\approx 10^{-7}$) than that observed by scanning tunneling spectroscopy,⁵ indicating that the existence of the gap feature beyond T_c essentially does not depend on R_J . The gap magnitude of $4\Delta(77.3 \text{ K}) = 98 \text{ meV}$ in Fig. 2 is slightly larger than 90 meV of Fig. 3 as already shown in Fig. 1 (A) and (C), but both are consistent with that of slightly overdoped regions.¹² With increasing the temperature, the zero-bias conductance (ZBC) (except the Josephson peak) increases smoothly across the bulk T_c at which the Josephson peak vanishes. The increase arises from the thermal filling up of the density of states inside the gap. The Josephson peak observed up to T_c is believed to be due to very clean interface of the SIS break junction. No sign of the gap-closing feature is seen even at T_c . Above T_c , the conductance inside the gap is still smoothly filling up on warming. The broadening feature of the gap in the superconducting state is smoothly connected with that above T_c . Most significantly, the gap structure of Fig. 2 eventually disappears at the characteristic temperature of $T^* \approx 185$ –190 K, remaining a broad zero-bias maximum in the background conductance. The thermal behavior of the gap having the slightly lower $T^* \approx 170$ K is presented in Fig. 3, demonstrating the reproducibility of the gap-closing temperature. In Fig. 3, the Josephson peak vanishes at $T_c = 84 \text{ K}$, and the inverse V -shaped background conductance is observed even below T_c . The temperature evolutions of Figs. 2 and 3 are almost similar to each other, while one could also consider that the $\approx 10 \text{ meV}$ reduction in

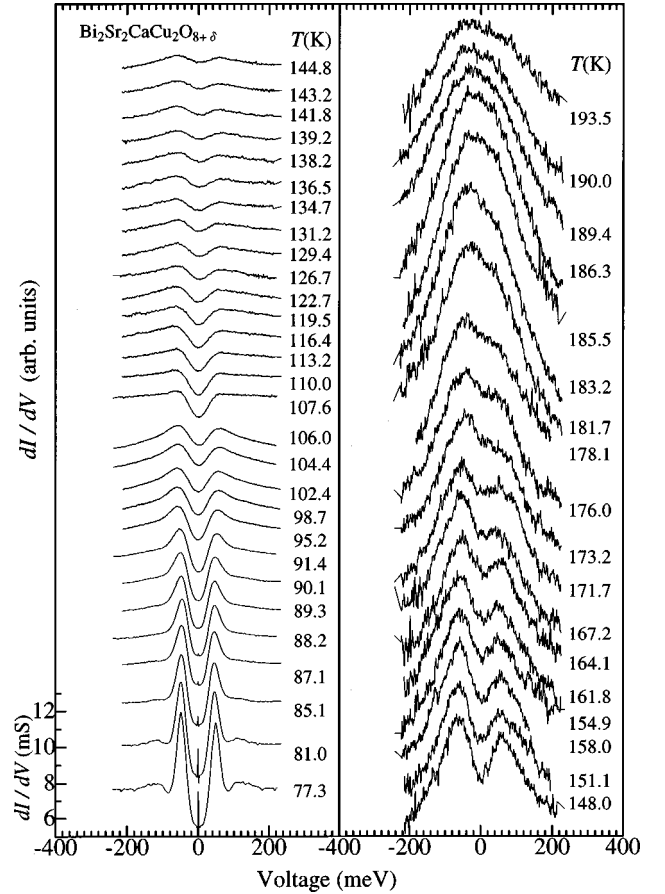


FIG. 2. Temperature variations of the tunneling conductance of Fig. 1 (A). The conductance scale corresponds to the 77.3 K spectrum, and the conductances are subsequently shifted up for the clarity.

$4\Delta(77.3 \text{ K})$ of Fig. 3 as compared with that of Fig. 2 would result in the $\approx 20 \text{ K}$ reduction of T^* . Figure 4 displays the dI/dV data from a different junction to demonstrate further the reproducibility of T^* using the sample batch no. 1. In this figure, the measurements were successful only above $\approx 170 \text{ K}$ after several readjustments of the bending force applying to the junction. The conductance possesses quite large leakage, in which the depth of the gap is less than 5% of the background. Nevertheless, we really see the gap structure which disappears at $T^* = 180 \text{ K}$ remaining the broad zero-bias maximum at least up to $\approx 290 \text{ K}$. This T^* value is in good agreement with that of Figs. 2 and 3. From the present reproducible results, we believe that the gap creation at $T^* \approx 170$ –190 K is rather a common phenomenon in as-grown Bi-2212 crystal. This also suggests the existence of a particular local phase in the Bi-2212 crystal with the present growth condition.⁹ Note here that the extremely high sensitivity with the cleanest interface of the SIS break junction is a key to success of probing a well-defined local (nonbulk) gap structure up to $\approx 200 \text{ K}$.

The existence of the broad zero-bias conductance maximum in Figs. 2–4 at high temperatures after disappearing of the gap structure seems to be common to the data which exhibit the gap feature above T_c . Since the width and magnitude of the broad background maximum are not so reproducible, their appearance is speculated to strongly depend on

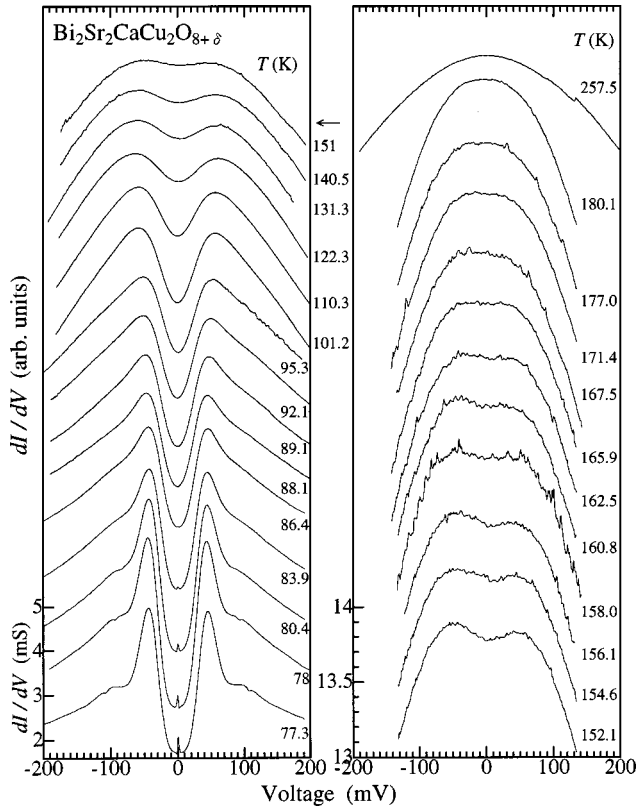


FIG. 3. Temperature variations of the tunneling conductance of Fig. 1 (C). The conductance scales of the left and right frames correspond to the 77.3 and 152.1 K spectra, respectively. The conductances are subsequently shifted up for the clarity.

the junction characteristics. Such a broad zero-bias maximum can be primarily due to the heating effect associated with the resistive state in the sample after the disappearance of the bulk superconductivity. This feature has been commonly observed in the nonsuperconducting tunnel junction.¹⁶ We should note that in Figs. 3 [Fig. 1 (C)] and 1 (B) it is observed even at 77.3 K. In this case inhomogeneous weak-link characteristics in the superconducting states may be responsible to the feature. We also suggest that the zero-bias maximum can be due to the Kondo or spin-flip scatterings of the conduction electrons with the bare magnetic moment of copper at the junction interface.¹⁷ It can be also explained in terms of the band structure effect such as van Hove singularity assuming the Fermi energy lying close to the singularity in the density of states.¹⁸ In any case we believe that the gap feature above T_c and the zero-bias maximum observed here does not correlate to each other.

The T^* values of ≈ 170 – 190 K of Figs. 2–4 in as-grown (slightly overdoped) crystals are almost consistent with those from PES⁴ and Josephson junction¹⁹ measurements, in which, however, the samples are believed to be in the underdoped region. The existence of such a high characteristic temperature has been also suggested by the bulk transport measurements.³ The temperature dependence of the resistance of our Bi-2212 measured by the break junction setup before the cracking process has sometimes shown either a weak irregularity or the onset of upturn at ≈ 160 – 180 K, but we cannot connect these structures with the present observations, because the resistance is not straightforward to obtain information about microscopic properties.

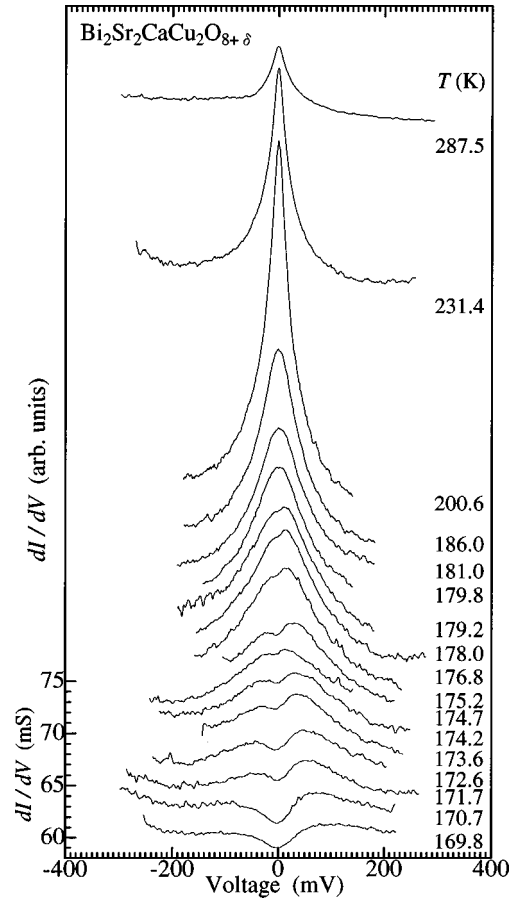


FIG. 4. Temperature variations of the tunneling conductance from as-grown $\text{Bi}_2\text{Sr}_2\text{CaCu}_2\text{O}_{8+\delta}$ (no. 1) break junction at high temperatures above ≈ 170 K. The conductance scale corresponds to the 169.8 K spectrum, and the conductances are subsequently shifted up for the clarity.

Figure 5 shows the temperature dependence of dI/dV presented in Fig. 1 (B). The gap magnitude of 4Δ (77.3 K) = 100 meV is the same as that of Fig. 2 [and Fig. 1 (A)], while the magnitude of the background conductance is $\approx 1/4$ of that of Fig. 2. The background conductance at 77.3 K showing an inverse V shape is similar to that of Fig. 3 [Fig. 1 (C)]. With increasing the temperature, the gap feature and Josephson peak gradually diminish. The latter disappears at the bulk $T_c = 85$ K, demonstrating the reproducible feature of its vanishment. Beyond T_c , the gap still exists like in Figs. 2 and 3, but it disappears quickly at a much lower temperature of $T^* \approx 107$ K, in spite of having the same gap magnitude as that of Fig. 2 at 77.3 K. This T^* value is very close to the T_c of the homologous superconductor $\text{Bi}_2\text{Sr}_2\text{Ca}_2\text{Cu}_3\text{O}_{10+\delta}$.²⁰ It is noted that the background conductance above T^* is very flat in contrast to that at 77.3 K and also that in Figs. 2–4, thereby showing the ideal metallic tunneling process.

In addition to very high-temperature gap structures which survive above T_c , we have also observed the conventional thermal behavior of the gap as shown in Fig. 6 [Fig. 1 (D)]. In this figure, the measurement starts at 10 K, and the gap structure and Josephson peak disappear simultaneously at $T_c \approx 90$ K. This feature is consistent with that of the nearly optimal doping region.¹² The value of 4Δ (77.9 K) ≈ 86 meV in Fig. 6 is slightly smaller than that of Figs. 2–4

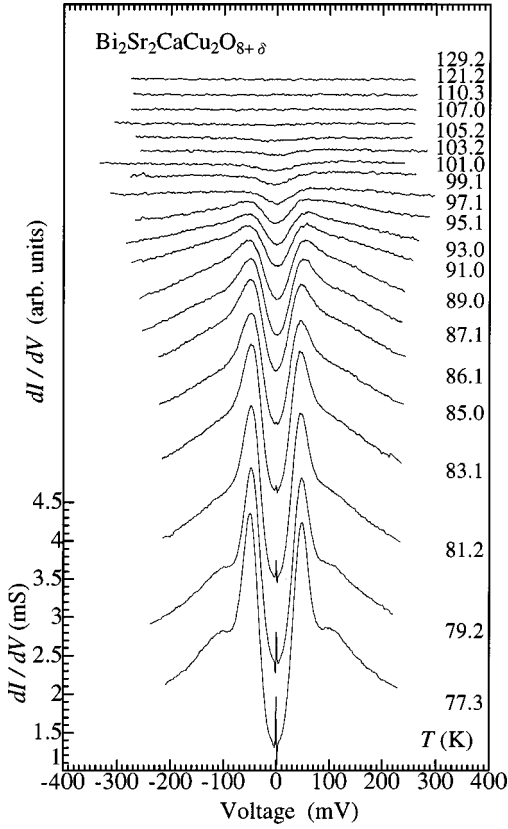


FIG. 5. Temperature variations of the tunneling conductance of Fig. 1 (B). The conductance scale corresponds to the 77.3 K spectrum, and the conductances are subsequently shifted up for the clarity.

(see Fig. 1), but it is in fact a small difference for the large difference in the gap-closing temperature between Fig. 6 (≈ 90 K) and Figs. 2–4 (≈ 170 – 190 K). Since R_J of Fig. 6 is much lower than that of Figs. 2–4, what we see in Fig. 6 might capture the different electronic states in the crystal from those of Figs. 2–4.

The temperature dependence of the gap magnitude $4\Delta(T)$ is plotted in Fig. 7 together with that of the zero-bias conductance (which is proportional to the thermally smeared density of states at the Fermi energy) normalized to the conductance at ± 150 mV. The frames (a) and (b) are taken from Figs. 2 and 3, respectively. The magnitude of $4\Delta(T)$ decreases with increasing the temperature up to T_c , then it turns to rapidly increase after taking a nonzero minimum at T_c . The $4\Delta(T)$ takes a maximum of ≈ 130 meV at ≈ 120 K, and smoothly decreases to disappear at $T^* \approx 170$ K (b)– 190 K (a). The increase of $4\Delta(T)$ with increasing the temperature from T_c up to ≈ 120 K in Fig. 7 cannot be explained solely by the thermal broadening of the BCS gap. This is because the ratio $\Delta(120\text{ K})/\Delta(90\text{ K}) \approx 1.4$ – 1.5 in this temperature interval is too large for the SIS junction, in which the change in the p - p separation is mostly due to the change in the gap edge which arises from the piling up of both the state-density singularities.⁸ Therefore, this must be due to the enhancement of the actual gap magnitude.

It might be considered that the broad zero-bias maximum in the background shown in Figs. 2–4 affects the thermal behavior of the gap feature. To clarify this point, we have

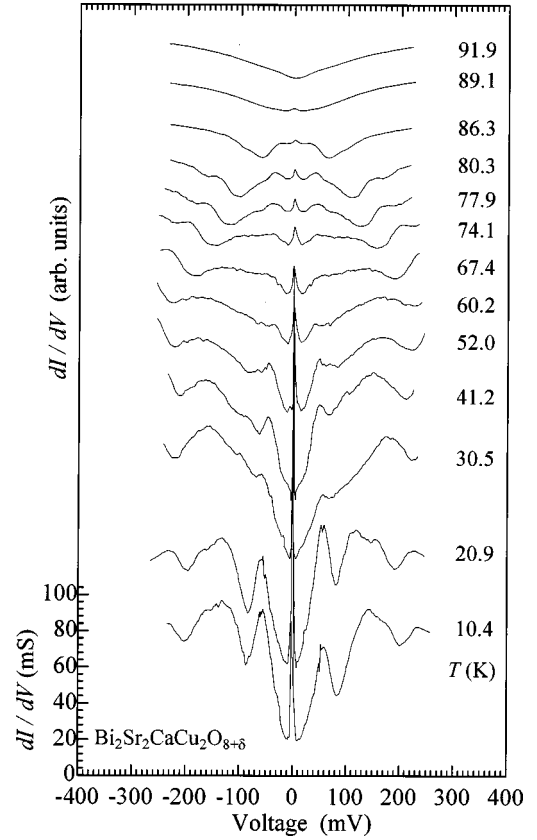


FIG. 6. Temperature variations of the tunneling conductance of Fig. 1 (D). The conductance scale corresponds to the 10.4 K spectrum, and the conductances are subsequently shifted up for the clarity.

numerically examined how the normal-state zero-bias maximum affects the p - p gap magnitude. The calculations using the thermal and lifetime broadened BCS density of states²¹ multiplied by a biquadratic function as the zero-bias maximum in the background showed that the narrowing of the p - p gap magnitude occurs when the actual gap decreases with increasing the temperature. In other words, the constant p - p gap magnitude against the temperature increase means the decrease of the actual gap magnitude because of the thermal broadening which usually enhances the p - p gap magnitude for the temperature-independent actual gap magnitude. Therefore we believe that the reduction of $\Delta(T)$ in Fig. 7 upon warming above ≈ 120 – 130 K is due to the decrease of the actual gap magnitude. We also note that the increase of $\Delta(T)$ with increasing the temperature between ≈ 85 – 120 K is never reproduced by considering such a zero-bias background maximum with a thermally constant gap.

The temperature dependence of the normalized zero-bias conductance NZBC(T) exhibits structures correlating with those of $\Delta(T)$. The overall magnitudes of NZBC(T) in Figs. 7(a) and 7(b) are very similar to each other. In Fig. 7(a), NZBC(T) increases steeply upon warming, displaying the changes in the slope at ≈ 120 K corresponding to the maximum temperature of $\Delta(T)$. It increases steeply again above 170 K, then it takes a peak around 190 K at which the gap structure disappears. This peak is probably due to a subtle change in the relative positions of both crystals on the break-junction substrate upon warming. The more convincing data are given in Fig. 7(b), where NZBC(T) rapidly in-

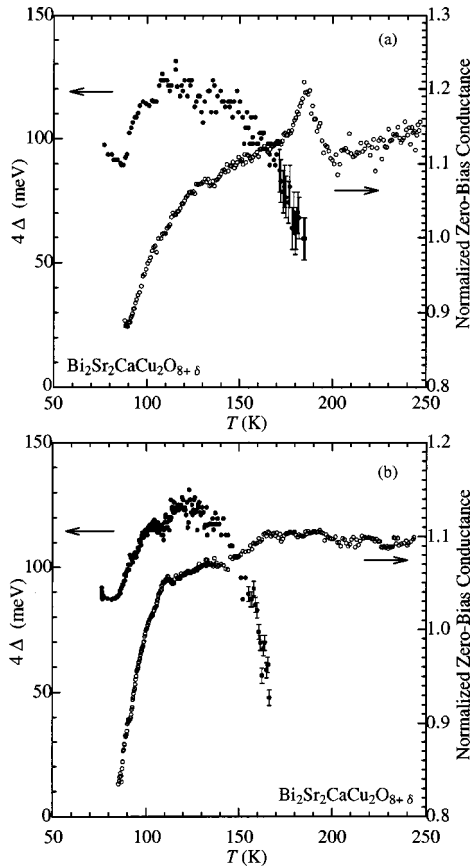


FIG. 7. Temperature dependence of the gap magnitude $4\Delta(T)$ and normalized zero-bias conductance. The data of (a) and (b) are taken from Figs. 2 and 3, respectively.

increases up to 110 K with increasing the temperature, then the increase becomes weak showing a kink at this temperature. At ≈ 130 K, there is another steplike structure which is close to the maximum temperature of $\Delta(T)$. This is similar to that of Fig. 7(a) occurring at ≈ 120 K. These structures indicate the successive filling up the states at the Fermi level. With further increasing the temperature, NZBC(T) still weakly increases, and then it shows a distinct kink at ≈ 170 K where the gap structure disappears. The NZBC(T) eventually levels off above this temperature. The feature of NZBC(T) near 170 K in Fig. 7(b) looks like the onset of the superconductivity in a conventional superconductor. In contrast to the behavior near 170–180 K, both $\Delta(T)$ and NZBC(T) between 85–120 K increase rather strongly with increasing the temperature, which qualitatively differs from the conventional behavior. The above characteristic temperatures of ≈ 120 –130 K and ≈ 170 –180 K have been also observed in the temperature dependence of the Knight-shift of the copper NMR measurements.²² We can roughly estimate the volume fractions of the gapped phase in Fig. 7(b) as $\approx 2\%$ at ≈ 110 K and $\approx 13\%$ at 86 K ($=T_c$) from the decrease in NZBC(T) assuming a convolution of the densities of states in the SIS junction. The nonmonotonous $\Delta(T)$ between 85–120 K as shown in Fig. 7, in which the gap is strongly influenced by the disappearance of the bulk superconductivity, is qualitatively different from the PES data, where the superconducting gap seems to smoothly merge into the normal-state gap.⁴ It is also in contrast to the simple

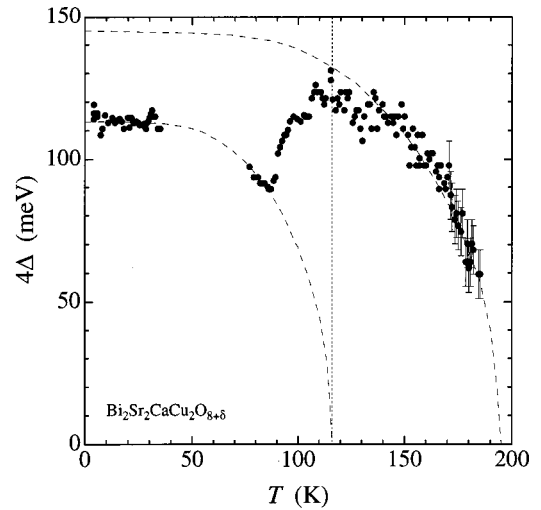


FIG. 8. Temperature dependence of the gap magnitude $4\Delta(T)$ from Fig. 2 together with the low-temperature data. The broken lines represent the BCS temperature dependence.

mean-field behavior of $\Delta(T)$ as an order parameter of the phase transition.²³

Figure 8 displays $4\Delta(T)$ from Fig. 2 [the same data as Fig. 7(a)] together with the low-temperature data to see Fig. 7(a) more quantitatively. Here the $\Delta(T)$ is fitted by the BCS prediction.²³ Clearly in the figure, the behavior of $4\Delta(T)$ cannot be fitted by a single BCS curve. We need two BCS curves to fit in the whole temperature range except for temperatures of ≈ 85 –130 K where the unusual behavior is observed. For the data below T_c , the temperature dependence of the gap magnitude can be fitted with $\Delta_1(0) = 28.3$ meV and the gap-closing temperature of $T^{*'} = 116$ K, while above 115 K, $\Delta_2(0) = 36.3$ meV and $T^* = 195$ K gives the best fitting. The extrapolated $\Delta_1(0)$ and $\Delta_2(0)$ are found to correspond to the gaps of slightly over and optimally doped regions,¹² respectively. The ratios $2\Delta_1(0)/k_B T^{*'} = 5.7$ and $2\Delta_2(0)/k_B T^* = 4.3$ from the above BCS extrapolated values are considerably reduced as compared with the ratios $2\Delta_1(0)/k_B T_c = 10.5$ or $2\Delta(0)/k_B T_c = 7.6$ [Fig. 1 (D)] using the actual T_c values, which agree with the commonly accepted ratio in the optimal or slightly overdoped crystals.¹² Interestingly, the extrapolated values of $T^{*'} = 116$ K corresponds to the temperature at which $4\Delta(T)$ takes a maximum as shown in Fig. 8. This suggests that the unusual behavior in the vicinity of T_c is a result of the competition between two kinds of gaps from different origins, where the superconducting gap persisting even at $T_c = 86$ K would completely disappear at ≈ 116 K if it were no gapping interaction which begins to develop above T_c . We can assume $T^{*'} = 116$ K as the local onset of the superconductivity from the fact that such a characteristic temperature really exists as T_c of $\text{Bi}_2\text{Sr}_2\text{Ca}_2\text{Cu}_3\text{O}_{8+\delta}$.²⁰ On the basis of this assumption, the observed thermal behavior can be explained as follows. With increasing the temperature the bulk superconducting order parameter of the Bi-2212 phase decreases, but above T_c at which the bulk superconductivity almost disappears, the gap magnitude from the higher temperature phase begins to recover against the residual local superconductivity. This recovery continues to $T^{*'} = 116$ K at

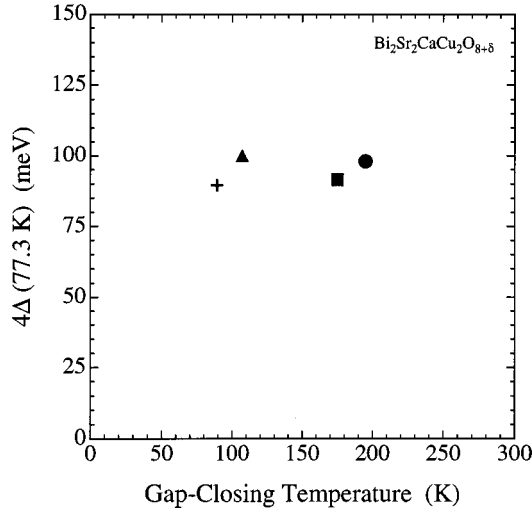


FIG. 9. The 4Δ (77.3 K) vs the Gap-closing temperature (T^* or T_c) using the data presented in this paper. Circle: Fig. 2; square: Fig. 3; triangle: Fig. 5; cross: Fig. 6.

which the local superconductivity is assumed to disappear. Above this temperature, only the gap from the much higher temperature phase is persisting up to ≈ 195 K. The complicated thermal behavior of the gap like this could be explained by considering the intergrowth structures consisting of the homologous $\text{Bi}_2\text{Sr}_2\text{Ca}_{n-1}\text{Cu}_n\text{O}_{2n+4+\delta}$ phases formed near the junction.²⁰ We note that in such structures a proximity effect between layers with different T_c 's near the junction might be responsible for producing an unusual temperature dependence of the gap.

There are other possible origins of the unusual behavior of $\Delta(T)$ as follows. The coexistence of charge-density wave (CDW) and superconductivity is predicted to yield unusual temperature dependence of the gap just like in the present observations, which strongly depends on the strength of the superexchange and Coulomb interactions.²⁴ A change in the gap symmetry at a characteristic temperature might modify the strength of the gapping interaction. More practically, a voltage drop across the bulk crystals with nonzero resistance state above T_c also could explain the upturn in $\Delta(T)$ at T_c .

The value of T^* apparently exceeds the range of T_c attained by the carrier doping in Bi-2212. It has been believed that the difference in the carrier doping level on the Bi-2212 phase diagram^{6,7} is responsible for the difference in the gap-closing temperature. In this view point, $T^* \approx 180$ K of the as-grown (slightly overdoped) crystal in Fig. 2 with $4\Delta(77.3\text{ K}) \approx 100$ meV is naturally expected to be lower than that of the underdoped sample with $4\Delta(4.2\text{ K}) \approx 180$ meV.⁵ However, as shown in Fig. 5, we have observed the similar gap feature of $4\Delta(77.3\text{ K}) = 98$ meV to that of Fig. 2 in as grown crystal with $T_c = 86$ K, which disappears at much lower temperature $T^* \approx 107$ K. This seems to be not consistent with the above argument of the doping difference. In Fig. 9, we plot $4\Delta(77.3\text{ K})$ versus T^* obtained from the present work. It is obvious that the gap at 77.3 K stays al-

most constant against the change in T^* about a factor of 2. This means that the gap feature above T_c does not correlate with the superconducting gap magnitude. Therefore, the change in T^* is not due to the change in the doping level as a bulk property, at least in our present observations. This is also consistent with the competing behavior of $\Delta(T)$ as shown in Figs. 7 and 8.

The origins of very high-temperature gap have been discussed in terms of either the precursor effect of the superconductivity^{6,7} or the non-superconducting effects.^{24,25,26} On the other hand, it seems to be not well understood experimentally whether it is an universal effect among the cuprates or a specific feature of Bi-2212.²⁷ From the viewpoint of the precursor effect, the gap feature beyond T_c can be associated with either the incoherent cooper-pairing due to superconducting phase fluctuation or the spin-singlet creation.^{6,7} Both predict no phase transition down to T_c , thus the gap feature above T_c is not considered to be an order parameter. Nevertheless, as shown in Fig. 8, the $\Delta(T)$ is well fitted by the BCS prediction in the restricted temperature range with a competing feature between the different kinds of gaps. Further, the characteristic temperatures in $\Delta(T)$ and NZBC(T) correlate well each other as shown in Fig. 7, indicating that the gapping condensation and the phase coherence set in simultaneously at T^* . We briefly describe the other possible origins of the observed anomalous high-temperature gap. They are given in terms of the incoherent antiferromagnetic correlations,²⁵ the CDW arising from the modulated incommensurate structure,^{15,28} the short range interaction,²⁴ or the charge stripes in the CuO_2 layer,²⁶ in which the resultant superperiodicities in the electronic structure would create the energy gap at high temperatures. These condensations, which might be competing with the superconductivity as a consequence of sharing the Fermi surface between the different gapping condensations, also could be responsible for the nonmonotonous temperature dependence of the gap, as already mentioned.²⁴

To summarize, we have observed the gap structures above T_c in as grown Bi-2212 crystals by the break junction. The gap-closing temperature T^* above T_c is found to be distributed as 110–190 K even in the same crystal batch with $T_c = 86$ –89 K having the same superconducting gap magnitudes. This distribution with the similar magnitudes of the superconducting gap indicates that the gap features of below and above T_c do not correlate with each other. The highest value of $T^* \approx 170$ –190 K is reproduced in numbers of junctions. This reproducibility among the scattered T^* suggests the existence of a particular local gapped phase near the junction. The observed thermal behavior of the gap with this highest T^* value cannot be described by a conventional manner, instead it is probably involved with the coexistence/competition of the different kinds of gaps. We believe on the basis of the present measurements that these features arise from the delicate local electronic structures which are able to be probed by *in situ* break junction with unaffected interface.

The authors acknowledge Professor K. Nagai for useful discussions.

- *Electronic address: ekino@ipc.hiroshima-u.ac.jp
 †Present address: Shimadzu Corp., Kyoto 604-8511, Japan.
- ¹H. Yasuoka, T. Imai, and T. Shimizu, in *Strong Correlation and Superconductivity*, edited by H. Fukuyama, S. Maekawa, and A. P. Malozemoff (Springer, New York, 1989).
 - ²J. Rossat-Mignod, L. P. Regnault, P. Bourges, C. Vettier, P. Bulet, and J. Y. Henry, *Physica B* **186-188**, 1 (1993).
 - ³B. Batlogg, H. Y. Hwang, H. Takagi, R. J. Cava, H. L. Kao, and J. Kwo, *Physica C* **235-240**, 130 (1994).
 - ⁴H. Ding, T. Yokota, J. C. Campuzano, T. Takahashi, M. Randeria, M. R. Norman, T. Mochiku, K. Kadowaki, and J. Giapintzakis, *Nature (London)* **382**, 51 (1996); A. G. Loeser, Z.-X. Shen, D. S. Dessau, D. D. Marshall, C. H. Park, P. Fournier, and A. Kapitulnik, *Science* **273**, 325 (1996).
 - ⁵Ch. Renner, B. Revaz, J.-Y. Genoud, K. Kadowaki, and Ø. Fischer, *Phys. Rev. Lett.* **80**, 149 (1998).
 - ⁶V. J. Emery and S. A. Kivelson, *Nature (London)* **374**, 434 (1995).
 - ⁷T. Tanamoto, K. Kohno, and H. Fukuyama, *J. Phys. Soc. Jpn.* **61**, 1886 (1992); G. Kotliar and J. Liu, *Phys. Rev. B* **37**, 3774 (1988).
 - ⁸E. L. Wolf, *Principles of Electron Tunneling Spectroscopy* (Oxford University Press, Oxford, 1989).
 - ⁹D. B. Mitzi, L. W. Lombardo, A. Kapitulnik, S. S. Laderman, and R. D. Jacowitz, *Phys. Rev. B* **41**, 6564 (1990).
 - ¹⁰H. Ding, A. F. Bellman, J. C. Campuzano, M. Randeria, M. R. Norman, T. Yokoya, T. Takahashi, H. Katayama-Yoshida, T. Mochiku, K. Kadowaki, G. Jennings, and G. P. Brivio, *Phys. Rev. Lett.* **76**, 1533 (1996); W. A. Groen *et al.*, *Physica C* **165**, 55 (1990).
 - ¹¹Y. Sezaki, T. Ekino, and H. Fujii, *Physica B* **259-261**, 555 (1999); T. Ekino, Y. Sezaki, and H. Fujii (unpublished).
 - ¹²N. Miyakawa, P. Guptasarma, J. F. Zasadzinski, D. G. Hinks, and K. E. Gray, *Phys. Rev. Lett.* **80**, 157 (1998).
 - ¹³D. Mandrus, L. Forro, D. Koller, and L. Mihaly, *Nature (London)* **351**, 460 (1991).
 - ¹⁴T. Ekino, T. Minami, H. Fujii, and J. Akimitsu, *Physica C* **235-240**, 1899 (1994).
 - ¹⁵T. Hasegawa and K. Kitazawa, *Jpn. J. Appl. Phys., Part 2* **29**, L434 (1990); M. Tanaka, T. Takahashi, H. Katayama-Yoshida, S. Yamazaki, M. Fujinami, Y. Okabe, W. Mizutani, M. Ono, and K. Kajmura, *Nature (London)* **339**, 691 (1989).
 - ¹⁶T. Ekino and J. Akimitsu, *Jpn. J. Appl. Phys., Suppl.* **26**, Suppl. 3, 625 (1987).
 - ¹⁷J. A. Applbaum and L. Y. L. Shen, *Phys. Rev. B* **5**, 544 (1972).
 - ¹⁸J. Bok and J. Bouvier, *Physica C* **274**, 1 (1997).
 - ¹⁹M. Suzuki, Y. Hidaka, K. Tanabe, S. Karimoto, and K. Namekawa, *Jpn. J. Appl. Phys., Part 2* **35**, L762 (1996).
 - ²⁰H. Maeda, Y. Tanaka, M. Fukutomi, and T. Adano, *Jpn. J. Appl. Phys., Part 2* **27**, L209 (1988).
 - ²¹R. C. Dynes, V. Narayanamurti, and J. P. Garno, *Phys. Rev. Lett.* **41**, 1509 (1978).
 - ²²K. Ishida, K. Yoshida, T. Mito, Y. Tokunaga, Y. Kitaoko, K. Asayama, Y. Nakayama, J. Shimoyama, and K. Kishio, *Phys. Rev. B* **58**, R5960 (1998).
 - ²³J. Bardeen, L. N. Cooper, and J. R. Schrieffer, *Phys. Rev.* **108**, 1175 (1957).
 - ²⁴M. V. Eremin, I. A. Lavinov, and S. V. Varlamov, *Physica B* **259-261**, 456 (1999).
 - ²⁵P. Aebi, J. Osterwalder, P. Schwaller, L. Schlapbach, M. Shimoda, T. Mochiku, and K. Kadowaki, *Phys. Rev. Lett.* **72**, 2757 (1994); **74**, 1886 (1995).
 - ²⁶See, for example, *Phys. Today* **51** (6), 19 (1998).
 - ²⁷We have also observed the high-temperature gap with $T^* \approx 160$ K in the homologous compound $(\text{Bi,Pb})_2\text{Sr}_2\text{Ca}_2\text{Cu}_3\text{O}_{10+\delta}$ [T. Ekino, Y. Sezaki, and H. Fujii, *Physica C* (to be published)].
 - ²⁸T. Matsui, H. Maeda, Y. Tanaka, E. Takayama-Muromachi, S. Takekawa, and S. Horiuchi, *Jpn. J. Appl. Phys., Part 2* **27**, L827 (1988).